

Comparative Performance Analysis of Gas Turbine with and without Intercooler using Natural Gas and Hydrogen Fuels

Asad Ali Sodhro

Department of Mechanical Engineering, Universiti Teknologi PETRONAS, Malaysia
asad_18003321@utp.edu.my (corresponding author)

Tamiru Alemu Lemma

Department of Mechanical Engineering, Universiti Teknologi PETRONAS, Malaysia
tamiru.lemma@utp.edu.my

Syed Ihtsham Ul-Haq Gilani

Department of Mechanical Engineering, Universiti Teknologi PETRONAS, Malaysia
syedihtsham@utp.edu.my

Waleligne Molla Salilew

Department of Mechanical Engineering, Universiti Teknologi PETRONAS, Malaysia
waleligne.salilew@utp.edu.my

Received: 27 August 2024 | Revised: 15 September 2024 | Accepted: 19 September 2024

Licensed under a CC-BY 4.0 license | Copyright (c) by the authors | DOI: <https://doi.org/10.48084/etasr.8825>

ABSTRACT

The Gas Turbine (GT) represents one of the most significant technological advancements of the early 20th century. A limited number of studies have explored the significance of intercooling in improving GT efficiency. Specifically, the comparative performance of GT utilizing Natural Gas (NG) and hydrogen fuel, with and without intercoolers, remains largely unexplored. In this study, design point and off-design performance models for a three-shaft GT were developed using commercial software. During the model development process, the intercooler was considered, as the GT was originally designed with an intercooler. The intercooler was subsequently deactivated to simulate the GT's performance with NG and without an intercooler. Following this analysis, the fuel type was switched to hydrogen to investigate the performance of the GT with and without an intercooler. The results indicate that the inclusion of an intercooler increases the power output from 75,176.8 kW to 99,000.2 kW for NG and from 75,012.2 kW to 99,001.6 kW for hydrogen. However, the thermal efficiency marginally decreases from 45.5% to 45.14% for NG and from 45.9% to 45.52% for hydrogen. These findings demonstrate that the intercooler enhances power output but results in a minor drop in efficiency. Furthermore, hydrogen consistently exhibits superior thermal efficiency and fuel consumption compared to NG in both scenarios.

Keywords-GT; intercooler; hydrogen fuel; NG

I. INTRODUCTION

The GT is a combustion engine that converts fuel into mechanical energy through the motion of its blades, enabling the turbine to generate power. Most GTs are designed to operate at higher pressure ratios. In such cases, an intercooler, functioning as a heat exchanger, is incorporated into these systems [1]. To reduce the temperature of the working fluid, the intercooler is placed between the Low-Pressure Compressor (LPC) and High-Pressure Compressor (HPC) to decrease the temperature and diminish the workload on the compressors [2]. Integrating this approach, specifically the addition of an

intercooler, into a GT cycle would lead to decreased fuel consumption. Consequently, this would result in an increase in the engine power output [3]. Thus, it is considered a beneficial technique for improving the overall efficiency of a GT cycle and reducing emissions [4]. However, when an intercooled heat exchanger is incorporated into a GT cycle, a reheating unit should be installed downstream of the compressor to compensate for the decrease in flow temperature. Furthermore, GTs equipped with intercooled systems are employed in various types of engines, including aero-engines, like the GE LMS 100, Siemens SGT-A65 engine, and marine engines, such

as the Westinghouse and Rolls-Royce WR-21 [5-7]. The intercooler design can accommodate either gas-gas or gas-liquid working fluids, with flow configurations, such as counterflow, parallel flow, or crossflow [8]. Additionally, there are two flows of working fluid that move perpendicularly to each other in a crossflow arrangement.

Relocating the intercooling within an intercooled-supercharged GT Brayton cycle on the efficiency of a supercharged GT system indicated that the mass-specific power and thermal efficiency were 20-30% higher than those of the traditional cycle [9]. A thermo-economic investigation of the intercooling cycle was carried out to determine the cost of GT cycles [10]. The impact of the intercooling cycle on emission performance was studied, providing a comprehensive analysis of the intercooled cycle [11]. However, the study lacks relevant research on integrating the guiding vane outlet and stator into a single blade to reduce system load and dimensions. The results indicate that the ideal specific heat ratio increases with the cycle pressure ratio, but efficiency can be improved by increasing the maximum temperature and total pressure ratios. A group of researchers developed a thermodynamic software model for an intercooled-cycle GT to study environmental factors and intercooler performance in relation to marine engine performance, using a MATLAB/Simulink-based nonlinear simulation model to identify optimal flow rates based on atmospheric and seawater conditions [12]. Furthermore, studying the thermodynamic cycle optimization of an intercooled turbofan engine, revealed that fuel consumption significantly depends on the height of intercooler fins, requiring optimal designs [13].

The existing literature has explored the performance of intercooling using NG and hydrogen fuels. However, the impact of intercooling on the performance of GTs remains understudied. This investigation aims to examine the influence of intercooling, either integrated in the presented system or not, on the performance of a three-shaft GT when operated with NG and hydrogen fuels. Figure 1 depicts the GT system under study comprises seven principal components.

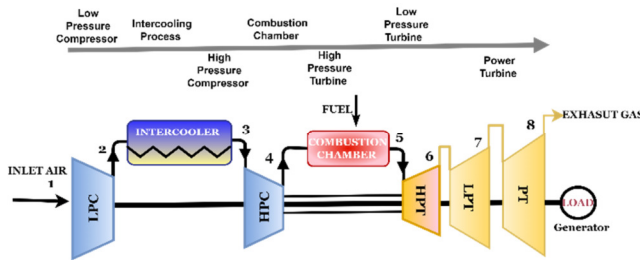


Fig. 1. Schematic of three shaft GT with stations and an intercooler.

II. DEVELOPMENT OF A GAS TURBINE PERFORMANCE MODEL

Developing design-point and off-design models is crucial for optimizing GT performance [14]. The design point model represents the engine's performance at the specified maximum designed load. From an off-design performance simulation perspective, the design point is viewed as a single operating

condition. By combining the individual component performances of the GT, the overall performance of the GT cycle can be determined [15]. The data utilized in the development of the design point model were sourced from the manufacturer's catalogue. To achieve accuracy and validate the obtained results, both the design point and off-design models were calculated using the energy balance and optimization techniques [16]. If the model's output matches the data provided by the manufacturer, then the model is considered reliable in terms of predicting engine performance [17].

A. Design Point Performance Modeling

The design point represents the optimal operating conditions of the GT, encompassing factors, such as inlet air conditions, rotational speed, and fuel flow rate. The input data consists of the ambient conditions, component efficiencies, compressor pressure ratio, mass flow rate, fuel-air ratio in the combustion chamber, and turbine inlet temperature. A performance model was created to determine the values of all unknown parameters at a specific operating point using thermodynamic equations. Evaluating the energy balance and compatibility of components that share a common shaft is crucial. A programming language, such as MATLAB or another suitable option, can be employed to develop the design point model. The design point performance model was developed by incorporating the input parameters obtained from the product data sheet and published literature [16]. The combustion chamber performance model was designed using the energy balance equation, taking into account pressure loss.

$$\dot{m}_a h_3 + \dot{m}_f \times LHV \times \eta_{CC} = (\dot{m}_a + \dot{m}_f) h_4 \quad (1)$$

$$\dot{m}_f = \frac{\dot{m}_a (h_4 + h_3)}{\eta_{CC} \times LHV - h_4} \quad (2)$$

$$W_{HPC} = W_{HPT} \quad (3)$$

$$W_{LPC} = W_{LPT} \quad (4)$$

$$W_{PT} = W_{Load} \quad (5)$$

where LHV indicates the lower heating value, η_{CC} is the combustion efficiency, \dot{m}_a is the inlet air mass flow rate, \dot{m}_f is the fuel mass flow rate, and h_3 is HPC outlet enthalpy, W_{LPC} is low-pressure compressor work, W_{HPC} is HPC work, W_{LPT} is high-pressure turbine work, W_{PT} is power turbine work, and W_{Load} is the load.

The validation conditions were achieved when the model was fully optimized. To conclude, the results of the design point model were compared to the design parameters provided in the gas turbine manufacturer. After examining the design point model output, it was concluded that the model closely matches the data provided by engine manufacturer, with only minor discrepancies.

B. Off-Design Performance Modeling

Following the successful completion of the cycle design point calculations, an off-design model was developed. The fundamental phase in off-design simulations entailed adjusting the target engine's design point using the specialized technique of scaling, in conjunction with the existing compressor and turbine mappings. The subsequent step in the off-design

process was component matching, which involved employing the iterative Newton-Raphson method to establish the compatibility between work and mass flow [14]. A steady-state off-design operating line is typically generated using the Newton-Raphson iterative method due to its efficacy in handling non-linear systems [18]. The off-design model was validated by comparing it to catalog data and the commercial software GasTurb 12. The power output as a function of ambient temperature was employed to verify the off-design model. In Figure 2, the power output exhibited a maximum variation of 0.002% with respect to ambient temperature at each operating point.

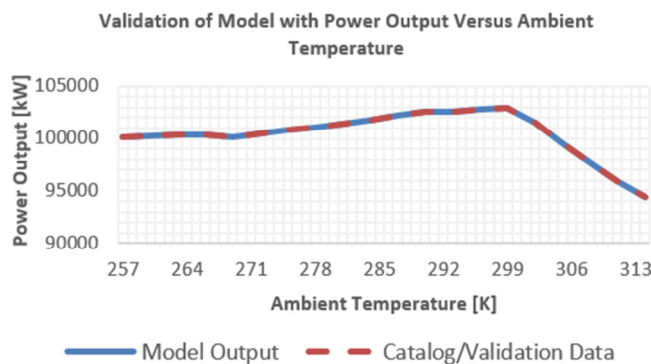


Fig. 2. Off-design model validation with the power output versus ambient temperature.

III. COMPARATIVE ANALYSIS

The parametric analysis on GT performance with and without an intercooler, utilizing NG and hydrogen as fuel sources, reveals that incorporating an intercooler significantly enhances power output and fuel flow rate for both fuels. Figure 3 shows the flow diagram of the followed procedure.

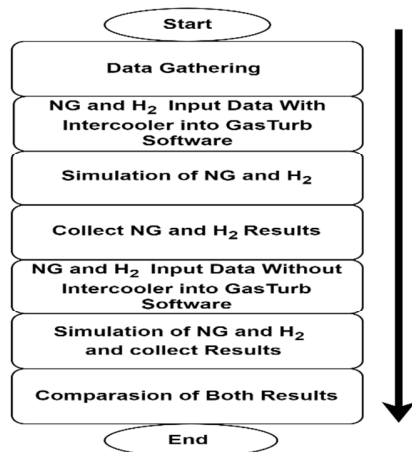


Fig. 3. Flow diagram of the comparative study.

Specifically, hydrogen power output increases from 75,012.2 kW to 99,001.6 kW, while NG power output rises from 75,176.8 kW to 99,000.2 kW. This improvement is attributed to the effect of intercooler cooling on the compressed air, enabling more effective combustion. However, this

enhancement is accompanied by a slight reduction in thermal efficiency, with hydrogen experiencing a 0.28% decrease and NG a 0.36% decrease. Additionally, the intercooler reduces exhaust temperatures and increases the heat rate, indicating improved fuel efficiency.

IV. RESULTS AND DISCUSSION

This study presents a comprehensive performance analysis of a system utilizing both NG and hydrogen fuels, with and without the incorporation of an intercooler. The analysis examines various performance parameters, including power output, thermal efficiency, power turbine exit temperature, heat rate, fuel flow rate, power-specific consumption, booster surge margin, and HPC surge margin, in relation to ambient temperature variations.

A. Effect of the Inclusion of an Intercooler on the Performance of GTs

A parametric study on a gas turbine engine with intercooler, operating on NG and hydrogen fuel, found that changing fuel type from NG to hydrogen led to a 0.37% deviation in thermal efficiency and a 187 kW power output deviation at lower temperatures. At higher temperatures, the deviation was 0.39% and the output was reduced to 73 kW. The average deviation in thermal efficiency at all ambient temperature points was 0.38%, and the average deviation in power output was 0.065%. Figure 4 shows that for both NG and hydrogen fuel, thermal efficiency and power output reduce linearly with increasing ambient temperature. At 243.15 K, NG had a thermal efficiency of around 46.75% and a power output of 1.25×10^5 kW. When using hydrogen, the efficiency was 47.12% and the power output was 1.23×10^5 kW. As the temperature rose to 315.15 K, NG efficiency dropped to 43.75% and the power output was 0.85×10^5 kW. Hydrogen efficiency decreased to 44.14% and the power output was 0.85×10^5 kW. The gas turbine efficiency increased when the fuel type was changed from NG to hydrogen due to three factors: flue gases, combustion fuel LHV, and turbine enthalpy reduction.

Figure 5 portrays the relationship between heat rate and power turbine exit temperature as a function of ambient temperature. At off-design conditions, at a lower temperature of 243.15 K, the change in the heat rate due to fuel switching was 61.16 kJ/kWh and the change in power turbine exit temperature was 2.07 K. At a higher temperature of 315.15 K, the change in the heat rate was 72.92 kJ/kWh and the change in the power turbine exit temperature was 2.08 K. The average change in the heat rate across the entire range of ambient temperature points was 66.17 kJ/kWh, and the average change in the power turbine exit temperature was 2.02 K. For both NG and hydrogen fuels, the heat rate and power turbine exit temperature increased with rising ambient temperature as indicated in Figure 5. At 243.15 K, NG had a heat rate of 7700 kJ/kWh, and a power turbine exit temperature of 661 K, while hydrogen had a heat rate of 7639 kJ/kWh and a power turbine exit temperature of 659 K. As the temperature increased to 315.15 K, NG's heat rate rose to 8227 kJ/kWh and the power turbine exit temperature to 679 K, whilst hydrogen's heat rate increased to 8154 kJ/kWh and the power turbine exit temperature to 677 K.

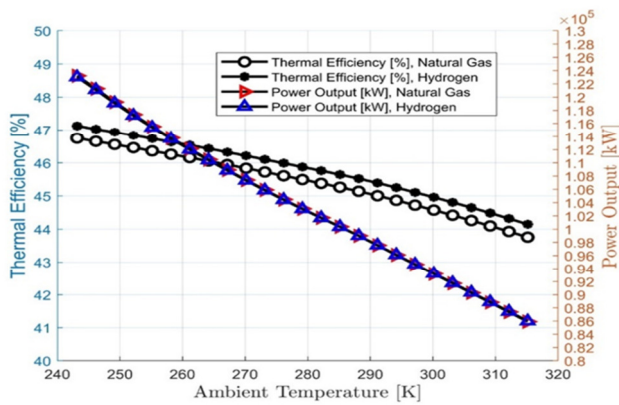


Fig. 4. Relationship between power output and thermal efficiency versus ambient temperature with intercooling for both NG and hydrogen fuel.

Figure 6 shows the relationship between fuel flow rate and power-specific fuel consumption as a function of ambient temperature for both NG and hydrogen fuels. At off-design conditions with a lower temperature of 243.15 K, the fuel flow deviation resulting from the fuel change from NG to hydrogen was 3.09 kg/s, and the deviation in power-specific fuel consumption was 0.9. At the higher temperature of 315.15 K, the fuel flow deviation was 2.3 kg/s, and the deviation in power-specific fuel consumption was 0.96. On average, the fuel flow deviation across the entire range of ambient temperatures was 2.67 kg/s, while the average deviation in power-specific fuel consumption was 0.93. The increasing ambient temperature leads to a decrease in fuel flow and a slight increase in power-specific fuel consumption for both NG and hydrogen fuels. At 243.15 K, the fuel flow for NG was 5.29 kg/s, and the power-specific fuel consumption was approximately 0.15, whereas for hydrogen, the fuel flow was about 2.20 kg/s, and the power-specific fuel consumption was 0.64. As the temperature increases to 315.15 K, the fuel flow for NG decreases to about 3.94 kg/s, and the power-specific fuel consumption is around 0.16, while for hydrogen, the fuel flow is about 1.64 kg/s, and the power-specific fuel consumption is approximately 0.68 kg/kWh.

The study examines the relationship between the surge margins of the HPC and the booster, and the ambient temperature, for both NG and hydrogen fuel is shown in Figure 7. The findings indicate that the transition from NG to hydrogen fuel led to a 0.2% deviation in the HPC surge margin at a lower temperature of 243.15 K, and a 0.11% deviation in the booster surge margin at a higher temperature of 315.15 K. The average deviation in the HPC surge margin across all ambient temperature points was 0.91%, while the average deviation in the booster surge margin was 0.37%. At 243.15 K and with the use of NG, the HPC surge margin was 23.13% and the booster surge margin was approximately 43.56%. When using hydrogen, the HPC surge margin was around 23.15% and the booster surge margin was 43.56%. As the temperature increases to 315.15 K, and with NG as the fuel, the HPC surge margin rises to about 24.22% and the booster surge margin is around 62.28%. In contrast, when using hydrogen, the HPC surge margin increases to 24.20% and the booster surge margin reaches approximately 62.28%.

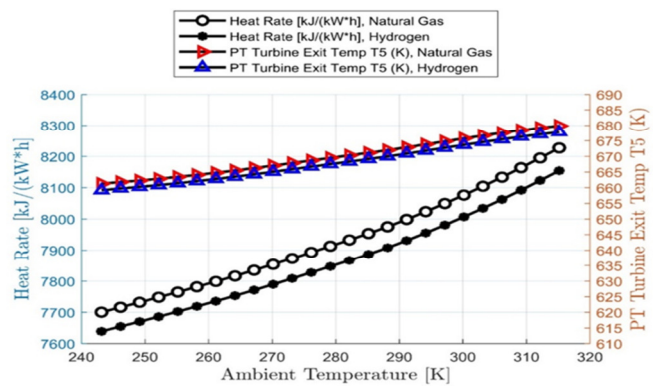


Fig. 5. Relationship between heat rate and power turbine exit temperature versus ambient temperature with intercooling for both NG and hydrogen fuels.

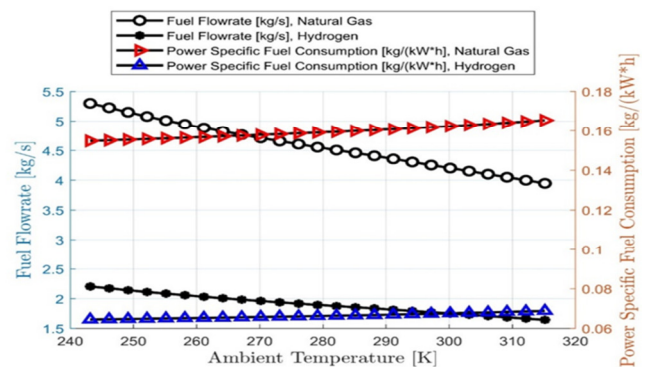


Fig. 6. Relationship between fuel flow rate and power specific fuel consumption versus ambient temperature with intercooling for both NG and hydrogen fuels.

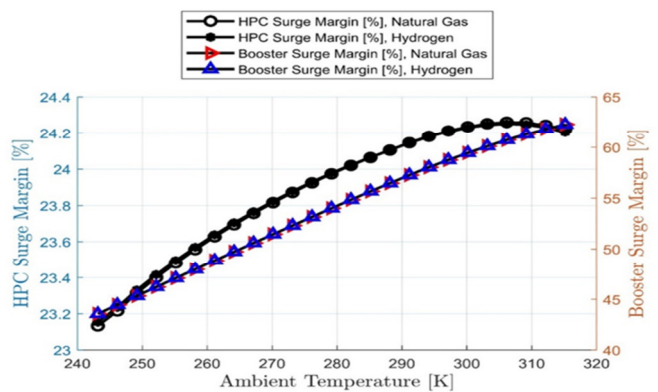


Fig. 7. Relationship between surge margins of HPC and booster versus ambient temperature with intercooling for both NG and hydrogen fuels.

B. Performance of a GT without Intercooler Addition

The results of the parametric study on a modeled GT engine without an intercooler, operated with NG and hydrogen fuel, are presented below. The parametric study investigated the impact of a temperature range from 243.15 to 315.15 K on thermal efficiency, power output, fuel flow rate, power-specific fuel consumption, heat rate, power turbine exit temperature, HPC surge margin, and booster surge margin. At off-design conditions with a lower temperature of 243.15 K, the thermal

efficiency deviation between NG and hydrogen fuel was 0.16%, and the power output deviation was 2798 kW. At a higher temperature of 315.15 K, the thermal efficiency deviation was 0.11%, and the power output deviation decreased to 4806 kW. The average deviation in thermal efficiency across the entire ambient temperature range was 2.55% when changing the fuel from NG to hydrogen, and the average deviation in power output was 3.03%.

Figure 8 exhibits that due to the absence of an intercooler, both fuels exhibited a linear reduction in thermal efficiency and power output as the ambient temperature increased. At 243.15 K, the thermal efficiency was approximately 46% and the power output was around 9.4×10^4 kW for NG, while for hydrogen, the thermal efficiency was about 45% and the power output was 9.1×10^4 kW. As the temperature rose to 315.15 K, the thermal efficiency dropped to around 43% and the power output decreased to approximately 6.0×10^4 kW for NG, whereas for hydrogen, the thermal efficiency decreased to approximately 44% and the power output to about 6.5×10^4 kW. The decrease in thermal efficiency for both fuels at higher temperatures was due to the reduced density of the air intake, resulting in less power generation and less efficient combustion. Compared to NG, hydrogen maintained better thermal efficiency but experienced a sharper decline in both efficiency and power output as the ambient temperature increased.

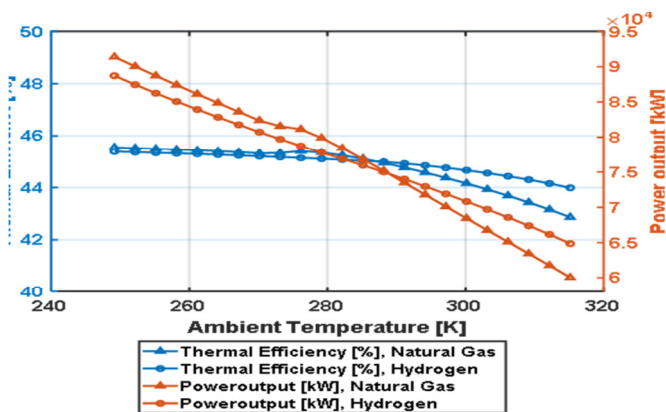


Fig. 8. Relationship between power output and thermal efficiency versus ambient temperature without intercooling for both NG and hydrogen fuels.

Figure 9 illustrates the relationship between heat rate and power turbine exit temperature as a function of ambient temperature. At the lower temperature of 243.15 K, the deviation in heat rate due to switching from NG to hydrogen fuel was 29.48 kJ/kWh, and the deviation in power turbine exit temperature was 3.27 K. At the higher temperature of 315.15 K, the deviation in heat rate was 215 kJ/kWh, and the deviation in power turbine exit temperature was 5.51 K. The average deviation of the heat rate across the entire range of ambient temperature was 59.46 kJ/kWh, and the average deviation in power turbine exit temperature was 2.97 K. The figure shows that for both fuels, heat rate and power turbine exit temperature increase with rising ambient temperature. At 243.15 K, the heat rate was 7893 kJ/kWh, and the power turbine exit temperature

was approximately 639.27 K when using NG, while with hydrogen the heat rate was about 7922 kJ/kWh and the power turbine exit temperature was 642.54 K. As the temperature increases to 315.15 K, the heat rate rises to around 8399 kJ/kWh and the power turbine exit temperature is approximately 705 K when using NG, whereas with hydrogen the heat rate increases to 8184 kJ/kWh and the power turbine exit temperature is about 699.33 K.

In Figure 10, at off-design conditions, with a lower temperature of 243.15 K, the difference in fuel flow rate due to the transition from NG to hydrogen was 2.45 kg/s, and the deviation in power-specific fuel consumption was 0.91 kg/kWh. At 315.15 K, the difference in fuel flow rate was 1.57 kg/s, and the deviation in power-specific fuel consumption was 0.997 kg/kWh. The change in the fuel type from NG to hydrogen resulted in an average deviation of 2.037 kg/s in the fuel flow rate and an average deviation of 0.93 kg/kWh in power-specific fuel consumption across the entire range of ambient temperature points. Figure 10 demonstrates that as the ambient temperature increases for both NG and hydrogen fuel, the fuel flow rate decreases, while the power-specific fuel consumption increases slightly. At 243.15 K, with the use of NG, the fuel flow rate was 4.14 kg/s, and the power-specific fuel consumption was approximately 0.15 kg/kWh. When using hydrogen as the fuel type, the fuel flow rate was around 1.7 kg/s, and the power-specific fuel consumption was 0.67 kg/kWh. As the temperature rises to 315.15 K, with NG as the fuel type, the fuel flow rate decreases to approximately 2.81 kg/s, and the power-specific fuel consumption is around 0.16 kg/kWh. In contrast, when using hydrogen, the fuel flow rate was about 1.24 kg/s, and the power-specific fuel consumption was around 0.997 kg/kWh. The analysis above demonstrates that as the temperature increases, the fuel flow rate decreases, and the power-specific fuel consumption increases with rising temperature.

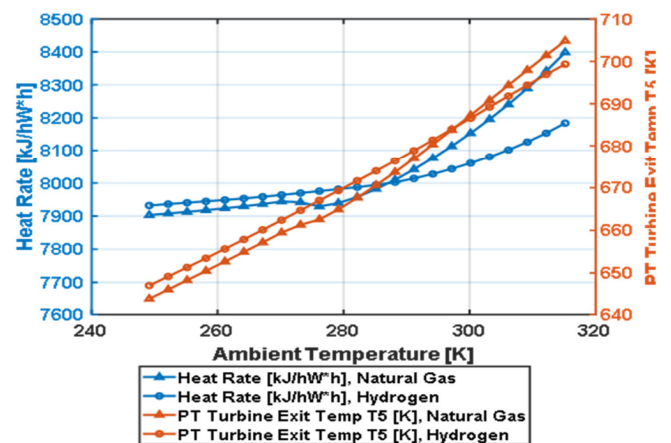


Fig. 9. Relationship between heat rate and power turbine exit temperature versus ambient temperature without intercooling for both NG and hydrogen fuels.

The current study examined the relationship between the surge margins of the HPC and booster as a function of ambient temperature for both NG and hydrogen fuels shown in Figure

11. At off-design conditions with a lower temperature of 243.15 K, the deviation in HPC surge margin when switching from NG to hydrogen fuel was 0.12%, while the deviation in booster surge margin was 10.48%. At a higher temperature of 315.15 K, the deviation in HPC surge margin was 0.25%, and the deviation in booster surge margin increased to 14.88%. The average deviation in HPC surge margin across the entire range of ambient temperatures was 0.115%, and the average deviation in booster surge margin was 12.65%. The results show that for both NG and hydrogen fuel, the HPC surge margin and booster surge margin increase linearly with increasing ambient temperature. At 243.15 K, the HPC surge margin was 24.29% and the booster surge margin was 50.31% for NG, while for hydrogen, the HPC surge margin was 24.41% and the booster surge margin was 60.80%. As the temperature increased to 315.15 K, the HPC surge margin increased to 27.37% and the booster surge margin decreased to 34.68% for NG, whereas for hydrogen, the HPC surge margin increased to 27.12% and the booster surge margin increased to 49.57%.

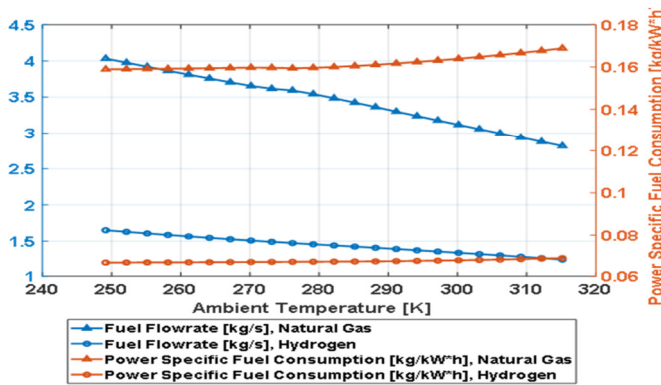


Fig. 10. Relationship between fuel flow rate and power specific fuel consumption versus ambient temperature without intercooling for both NG and hydrogen fuels.

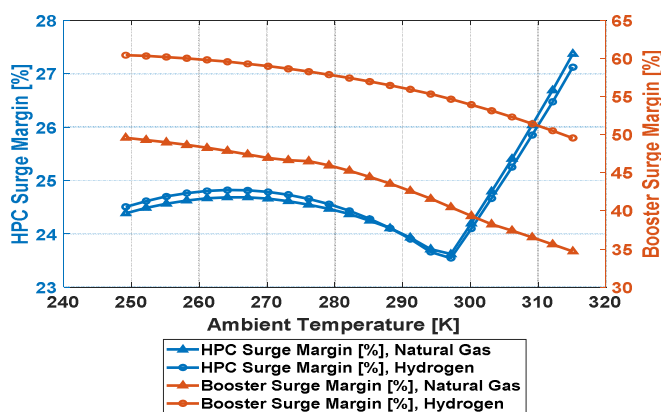


Fig. 11. Relationship between surge margins of HPC and booster versus ambient temperature for both NG and hydrogen fuels.

V. CONCLUSIONS

The paper examines the effects of employing Natural Gas (NG) and hydrogen fuel on the performance of a three-shaft industrial Gas Turbine (GT), with and without an intercooler. The findings indicate that integrating an intercooler into a three-shaft GT significantly enhances the power output, from 75,176.8 to 99,001.6 kW for NG, and from 75,012.2 to 99,001.6 kW for hydrogen. Nevertheless, this power increase results in reduced thermal efficiency, with NG efficiency decreasing from 45.5% to 45.14% and hydrogen from 45.9% to 45.52%. Consistently, hydrogen fuel demonstrates improved thermal performance and fuel efficiency compared to NG. Therefore, adding an intercooler improves overall turbine performance, while hydrogen fuel provides better efficiency and reduces fuel consumption. Further research should focus on enhancing intercooler designs and configurations to achieve better efficiency, as well as exploring alternative fuel blends to augment overall performance and sustainability in three-shaft industrial GTs.

ACKNOWLEDGMENT

Authors are thankful to Universiti Teknologi PETRONAS, Malaysia for providing the tools and resources required for this research project.

REFERENCES

- [1] A. Ali, M. Houda, A. Waqar, M. B. Khan, A. Deifalla, and O. Benjeddou, "A review on application of hydrogen in gas turbines with intercooler adjustments," *Results in Engineering*, vol. 22, Jun. 2024, Art. no. 101979, <https://doi.org/10.1016/j.rineng.2024.101979>.
- [2] A. M. Y. Razak, "Gas turbine performance modelling, analysis and optimisation," in *Modern Gas Turbine Systems*, Ed. Woodhead Publishing, 2013, pp. 423–514.
- [3] A. E. S. E. T. Alajmi, N. M. Adam, A. A. Hairuddin, and L. C. Abdullah, "Fuel atomization in gas turbines: A review of novel technology," *International Journal of Energy Research*, vol. 43, no. 8, pp. 3166–3181, 2019, <https://doi.org/10.1002/er.4415>.
- [4] B. Zohuri and P. McDaniel, *Combined Cycle Driven Efficiency for Next Generation Nuclear Power Plants*, 2nd ed. Cham, Switzerland: Springer International Publishing, 2018.
- [5] J. H. Jeong, L. S. Kim, J. K. Lee, M. Y. Ha, K. S. Kim, and Y. C. Ahn, "Review of Heat Exchanger Studies for High-Efficiency Gas Turbines," in *Proceedings of ASME Turbo Expo 2007: Power for Land, Sea, and Air*, Montreal, Canada, Mar. 2009, pp. 833–840, <https://doi.org/10.1115/GT2007-28071>.
- [6] U. Schütz, "New Mobile Gas Turbine with a Wide Range of Applications," *Mechanical Engineering*, vol. 140, no. 03, Mar. 2018, <https://doi.org/10.1115/1.2018-MAR-9>.
- [7] S. B. Shepard, T. L. Bowen, and J. M. Chiprich, "Design and Development of the WR-21 Intercooled Recuperated (ICR) Marine Gas Turbine," in *Proceedings of ASME 1994 International Gas Turbine and Aeroengine Congress and Exposition*, The Hague, Netherlands, Feb. 2015, <https://doi.org/10.1115/94-GT-079>.
- [8] P. Jansohn, *Modern Gas Turbine Systems High Efficiency, Low Emission, Fuel Flexible Power Generation*, 20th ed. Cambridge, UK: Woodhead Publishing Limited, 2013.
- [9] L.-S. Wang, "Optimum Peak Cycle Pressure for the Intercooled-Supercharged Gas Turbine Engine," *American Society of Mechanical Engineers*, vol. 2, 1995.
- [10] M. Sahu, T. Choudhary, and Y. Sanjay, "Thermoeconomic Investigation of Different Gas Turbine Cycle Configurations for Marine Application," *Society of Automobile Engineers*, no. 2228, Oct. 2016, <https://doi.org/10.4271/2016-01-2228>.

- [11] A. Kumari and Sanjay, "Investigation of parameters affecting exergy and emission performance of basic and intercooled gas turbine cycles," *Energy*, vol. 90, no. 1, pp. 525–536, Oct. 2015, <https://doi.org/10.1016/j.energy.2015.07.084>.
- [12] Y. Ying, Y. Cao, S. Li, and Z. Wang, "Study on flow parameters optimisation for marine gas turbine intercooler system based on simulation experiment," *International Journal of Computer Applications in Technology*, vol. 47, no. 1, 2013, <https://doi.org/10.1504/IJCAT.2013.054302>.
- [13] T. Ito, S. Teramoto, and K. Okamoto, "Effects of Heat Exchanger Characteristics on Optimized Intercooled Turbofan Engine Cycles," *International Journal of Gas Turbine, Propulsion and Power Systems*, vol. 6, no. 3, pp. 16–22, 2014, https://doi.org/10.38036/jgpp.6.3_16.
- [14] M. B. Hashmi, T. A. Lemma, and Z. A. Abdul Karim, "Investigation of the Combined Effect of Variable Inlet Guide Vane Drift, Fouling, and Inlet Air Cooling on Gas Turbine Performance," *Entropy*, vol. 21, no. 12, Dec. 2019, Art. no. 1186, <https://doi.org/10.3390/e21121186>.
- [15] A. M. Y. Razak, *Industrial Gas Turbines Performance and Operability*, 1st ed. Cambridge, UK: Woodhead Publishing Limited, 2007.
- [16] J. Ghojel, "Design-Point Calculations of Industrial Gas Turbines," in *Fundamentals of Heat Engines*, 1st ed., United Kingdom: John Wiley & Sons Ltd and ASME Press, 2020, pp. 376–394.
- [17] A. Nasir, A. Mohammed, and J. Y. Jiya, "Design and Off-Design Operation and Performance Analysis of a Gas Turbine," in *Proceedings of the World Congress on Engineering 2018*, London, UK, Jul. 2018, vol. 2.
- [18] W. M. Salilew, Z. A. Abdul Karim, T. A. Lemma, A. D. Fentaye, and K. G. Kyprianidis, "Three Shaft Industrial Gas Turbine Transient Performance Analysis," *Sensors*, vol. 23, no. 4, Jan. 2023, Art. no. 1767, <https://doi.org/10.3390/s23041767>.
- [19] T. H. Stuen, "Influence of Hydrogen Use As a Fuel on Aeroderivative Gas Turbine Performance," Master Thesis, Norwegian University of Science and Technology, Trondheim, Norway, 2021.
- [20] R. Agbadede, B. Nkoi, and B. Kainga, "Performance Analysis of Industrial Gas Turbines Fueled with Hydrogen," *Nigerian Research Journal of Engineering and Environmental Sciences*, vol. 5, no. 1, pp. 178–189, Jun. 2020.